

## Locating Graves in Different Soil Types and Burial Ages in Pulau Pinang using Ground Penetrating Radar

(Mengesan Kubur dalam Pelbagai Jenis Tanah dan Umur Perkuburan di Pulau Pinang menggunakan Radar Tusukan Bumi)

IFFAH ZALIKHA ROSLAN, MUHAMAD HAFIZUDDIN MOHD MANSOR, NAJMIAH ROSLI, NABILAH HUSNA  
ABDULLAH SANUSI & NUR AZWIN ISMAIL\*

### ABSTRACT

*Ground-penetration radar (GPR) is a geophysical tool widely applied in archaeological and forensic research, such as identifying the exact position of graves. A detailed GPR survey was conducted on the cemeteries in Permatang Pasir and Titi Teras, Penang Island. Moving a 500 MHz GPR antenna along parallel transects inside grids was used to collect data. The study's aim was to present two case studies with varying soil types and burial ages. Analysis of reflection shape, reflection strength and signal polarity helped in the interpretation of burial anomalies. The results varied depending on the soil type; in the sandy field, the GPR investigations were clearer and less complicated than in the clayey sand field. When the conditions are ideal (low conductivity areas with little vegetation), GPR provides highly informative and precise results. Time-slices representations were used as a method to provide details about the subsurface reflection at a certain depth.*

*Keywords: Burial ages; GPR; graves; soil type; time-slices*

### ABSTRAK

*Radar tusukan bumi (GPR) adalah alat geofizik yang banyak digunakan dalam penyelidikan arkeologi dan forensik, seperti mengenal pasti kedudukan kubur yang tepat. Tinjauan GPR secara terperinci dilakukan di tanah perkuburan di Permatang Pasir dan Titi Teras, Pulau Pinang. Menggerakkan antena GPR 500 MHz di sepanjang transek selari dalam grid digunakan untuk mengumpulkan data. Tujuan kajian ini adalah untuk mengemukakan dua kajian kes dalam pelbagai jenis tanah dan usia perkuburan. Analisis bentuk pantulan, kekuatan pantulan dan kekutuban isyarat membantu dalam penafsiran anomali perkuburan. Hasilnya berbeza-beza bergantung kepada jenis tanah; di kawasan berpasir, kajian GPR lebih jelas dan kurang rumit daripada di kawasan pasir berlumpur. Apabila keadaannya sesuai (persekitaran kekonduksian rendah dengan sedikit tumbuh-tumbuhan), GPR memberikan hasil yang sangat bermaklumat dan tepat. Hirisan masa digunakan sebagai kaedah untuk memberikan perincian mengenai pantulan permukaan bawah tanah pada kedalaman tertentu.*

*Kata kunci: GPR; hirisan masa; jenis tanah; kubur; umur perkuburan*

### INTRODUCTION

Ground-penetrating radar (GPR) has been useful for the exploration of archaeological since the 1990s (Mellett 1992). The most widely used GPR survey is to find unmarked graves (Bellantoni 2010; Bevan 1991; Conyers 2006; Davis et al. 2000; Doolittle & Hansen et al. 2014; Fiedler et al. 2009; Gaffney et al. 2015; Nobes 1999; Vaughan 1986; Widodo et al. 2016). GPR surveys are recently also used in forensic investigation, for instance

in the detection and search of possible forensic material hidden for individual and mass graves for murder victims (Nobes 2000; Ruffell 2005; Schultz 2007).

GPR is a non-destructive, comparatively high-resolution geophysical instrument used in archaeological investigation to explore underground object. GPR signals may be used to determine grave characteristic such as burial depth, size, coffin type, orientation, and burial quantity in a specific area. The effectiveness of GPR system

to detect human burials affected significantly by soil types. Electromagnetic wave (EM) velocity varies with soil type, operation frequencies and moisture content (Nazli et al. 2010). The permittivity of soil affects the propagation velocity of EM wave (Baker et al. 2007). Thus, the human burial reflected signal is affected by the reflection coefficient between soil and human burial. The greater the relative permittivity of two media, the greater the reflected signal in the GPR (Fiedler et al. 2009). According to Damiata et al. (2013), unmarked graves can be identified when there is a difference between two media. For example, bone and backfill material (skeletal remains), fleshly body tissues and the disturbed soil materials (body decomposition) and void spaces inside the burial feature.

Modern graves are ideal for evaluating the precision of the GPR survey in the detection of graves. The study aims to investigate the applicability of using GPR in detecting graves in different types of soil (sandy and sandy clay). The second aim of this paper was to study the GPR signal on known burial ages. The detail is focused on the reflection shape, reflection strength and signal polarity.

#### GPR PRINCIPLE

Ground-penetrating radar employs electromagnetic waves (EM) at a very high rate to map the subsurface of interest. The EM wave is emitted from the transmitter into the subsurface, reflected at an interface or scatters point sources and recorded by the receiving antenna. The EM wave propagation velocity and the reflection strength are determined by relative permittivity contrast between two media. The relative permittivity defines the ability of the medium to store and release EM energy relative to the corresponding ability of a vacuum (Annan 2009).

The relative permittivity ( $\epsilon_r$ ) defines the GPR radar velocity in the low loss materials (Annan 2009) given by (1):

$$v = \frac{c}{\sqrt{\epsilon_r}} \quad (1)$$

where  $v$  is the radar velocity, and  $c$  is the speed of light in vacuum ( $3 \times 10^8 \text{ ms}^{-1}$ ) and the signal wavelength  $\lambda$  (m) in the medium is given by (2):

$$\lambda = \frac{v}{f_c} \quad (2)$$

where  $f_c$  is the center frequency (Hz) of the antenna (Annan 2009).

The reflection strength is a measure of differences in relative permittivity between two adjacent media (Neal 2004). The reflection strength is also known as the reflection coefficient which expressed by the following (3):

$$R = \frac{(\sqrt{\epsilon_{r2}} - \sqrt{\epsilon_{r1}})}{(\sqrt{\epsilon_{r1}} + \sqrt{\epsilon_{r2}})} \quad (3)$$

where  $\epsilon_{r1}$  and  $\epsilon_{r2}$  are the relative permittivity of the upper and lower (or embedded) materials, respectively. The greater the value of the reflection coefficient, the greater energy is reflected.

The permittivity contrast between two media at the interface will determine the positive and negative of the reflection polarity (Annan 2003; Neal 2004). A positive reflection coefficient means that the pulse has normal banding polarity (white-black-white) when or  $v_2 < v_1$ . Conversely, a negative reflection coefficient has banded with reverse polarity (black-white-black) means that the reflected signal goes through a phase shift of  $180^\circ$ , which when or  $v_2 > v_1$ .

#### STUDY AREA

The study areas are selected based on the different types of soil in Penang Island to achieve reliable and acceptable results. Two study areas were selected for this study which was Kampung Permatang Pasir Cemetery and Kampung Titi Teras Cemetery. Both of the study areas area is located in Balik Pulau, southwest of Penang Island, Penang, Malaysia. Penang Island area is underlain by igneous rocks known as granites. In the southern half of the Penang Island, the type of granite is medium to coarse-grained megacrystic muscovite-biotite granite represented by late Triassic to early Jurassic. Balik Pulau is underlain by the Gula Formation composed of silt, clay, sand, gravel, and peat (Hassan 1990) (Figure 1).

Kampung Permatang Pasir is located approximately at latitude  $5.372743^\circ \text{ N}$  and longitude  $100.210765^\circ \text{ E}$  (Figure 2(a)). The top of the study area is surrounded by sandy soil. The study area was directly exposed to the light and the soil was clear of vegetation (Figure 2(b)). The cemetery features a semi-systematic grave layout.

The coordinate for Kampung Titi Teras Cemetery is  $5.354610^\circ \text{ N}$  and longitude  $100.224596^\circ \text{ E}$  (Figure 3(a)). The study area is dominated by sandy clay soil, small hills, grassy areas, and large trees (Figure 3(b)). The cemetery is scattered layout. To mark the location of graves, tombstones are commonly positioned at both ends of the grave; head and toe. The age of burials is determined by the marker on the tombstones and some tombstones are unmarked.

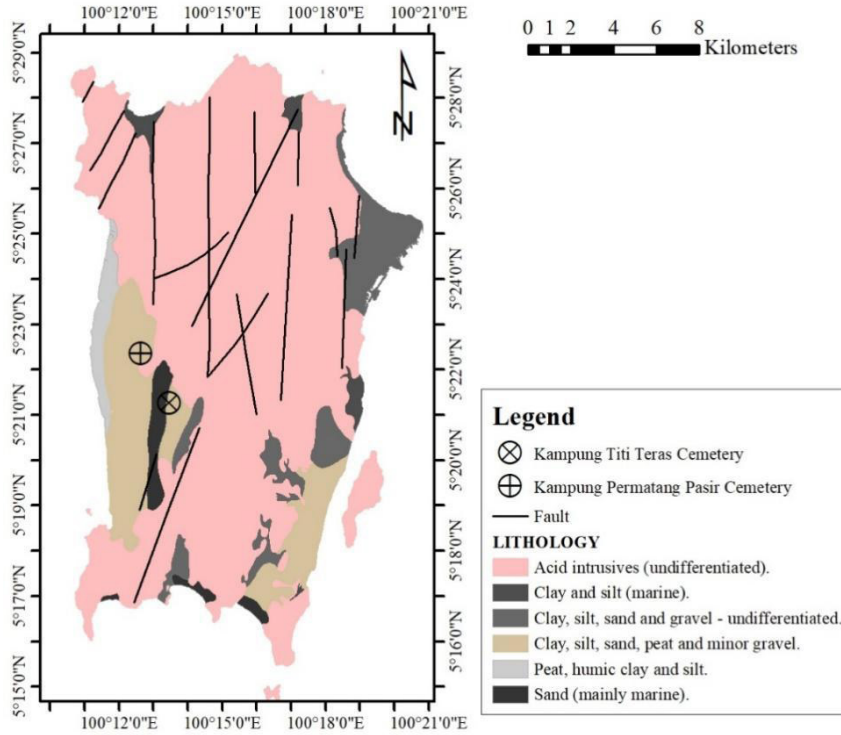


FIGURE 1. Geological map of the study area

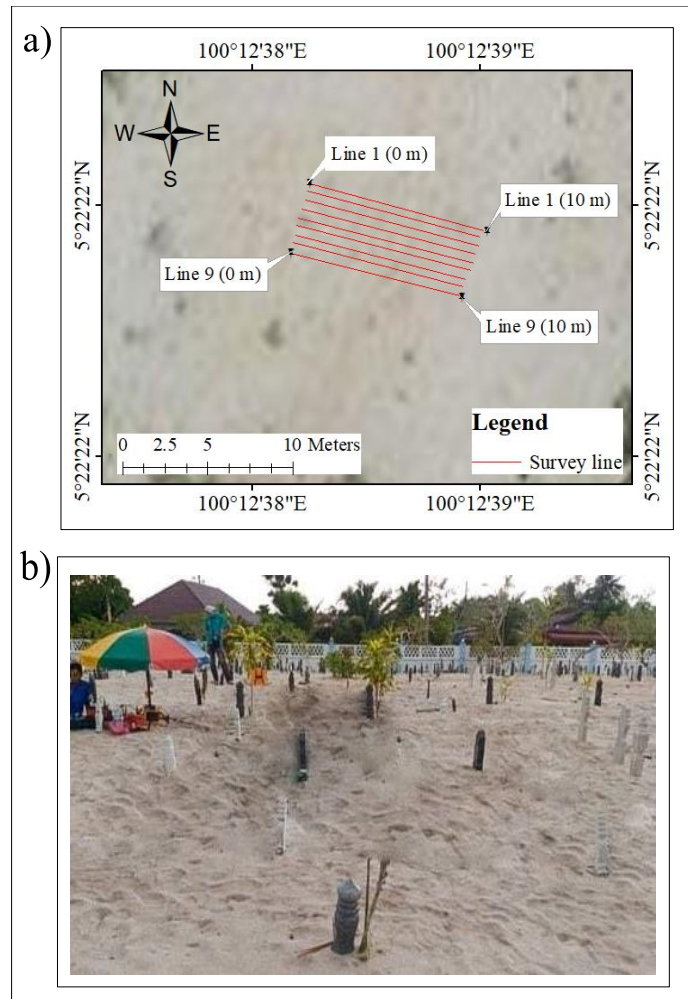


FIGURE 2. a) Location of GPR profiles on Permatang Pasir cemetery b) Photograph of site

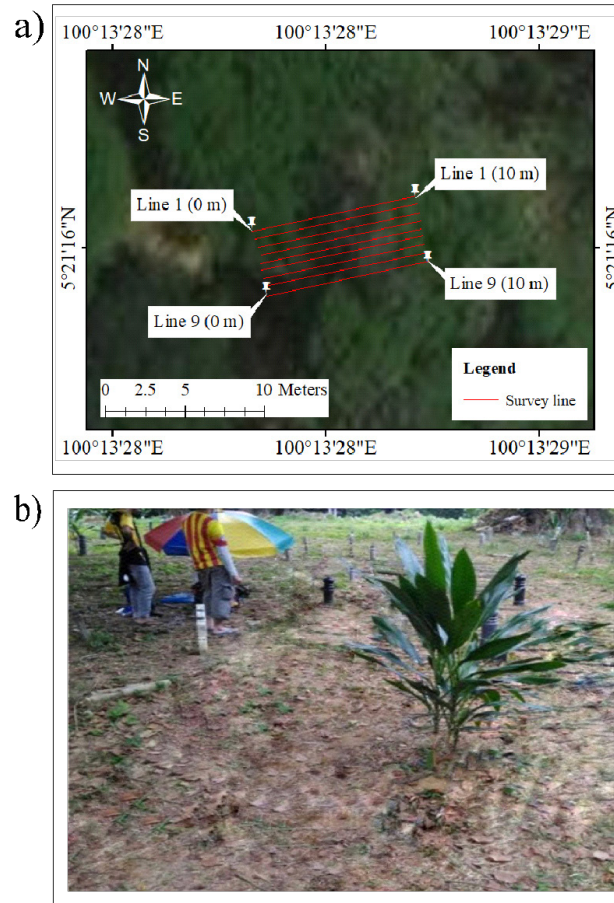


FIGURE 3. a) Location of GPR profiles on Permatang Pasir cemetery b) Photograph of site

#### MATERIALS AND METHODS

The study relied on laboratory work as well as a ground penetrating radar survey. Undisturbed soil samples were collected from the Permatang Pasir and Titi Teras cemeteries. The particle size distribution (PSD) analysis was then carried out, and soil classification was obtained. The RAMAC (Mala Geoscience, Mala, Sweden) radar device with a shielded antenna of 500 MH was used to conduct GPR survey on the Permatang Pasir and Titi Teras. In Permatang Pasir, 9 GPR survey lines of 10 m length each were carried out. Moreover, the separation distance between lines in this survey was set to 0.5 m (Figure 4). The GPR antenna was positioned perpendicular to existing eight marked graves. Since only one tombstones was found in study field, the exact orientation of grave G4 is unknown. The burial anomalies were classified into three groups: young (<5 years) (G2,

G3), intermediate ( $5 < x < 50$  years) (G7, G8) and old (>50 years) (G1, G4, G5, G6).

In Titi Teras (Figure 5), 9 survey lines of 10 m length and 0.5 m line spacing were carried out. Within 9 survey lines, four graves were identified and one grave (G1) whose exact orientation is unknown. The burials are divided into 2 classes which are young (<5 years) (G3, G4, G5) and old (>50 years) (G1, G2).

Following data acquisition, the GPR signals were processed and analyzed using the Sandmeier™ ReflexW v.7 software. GPR data can be interpreted in 2-D and 3-D using the software. The reflection shapes (hyperbola or planar reflection) and amplitude traces can be detected using a 2-D radargram. The radargram shows the result of a GPR survey conducted along the traverses. The vertical axis on the radargram represents the two-way travel time in nanoseconds (ns) or depth in metre (m).

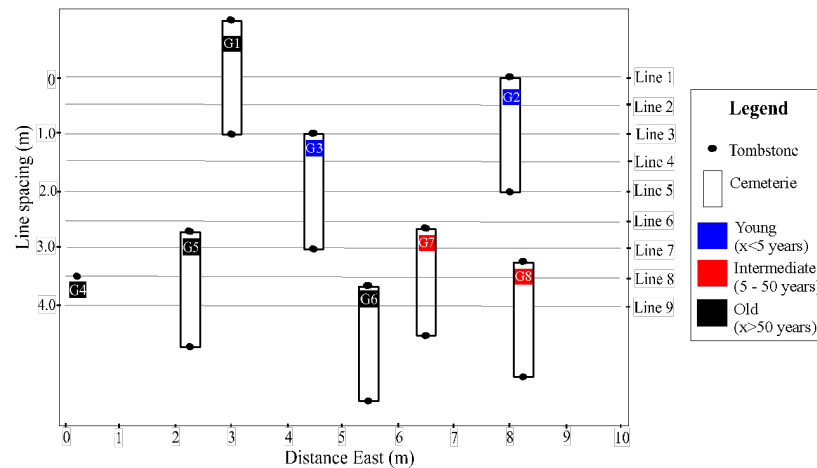


FIGURE 4. Survey lines of eight marked graves with different burial ages

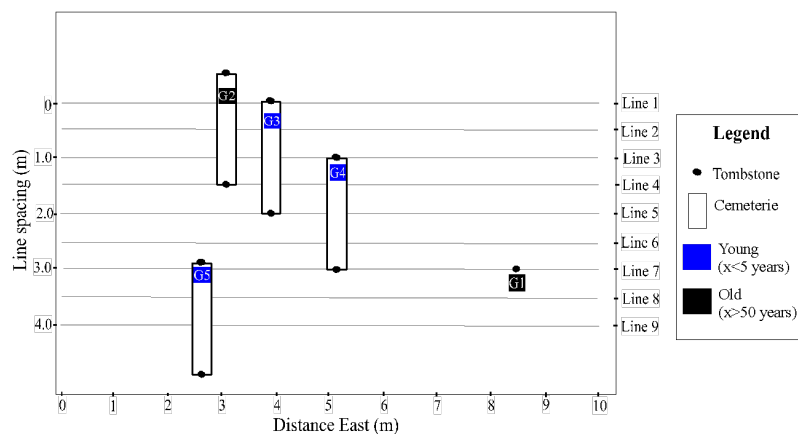


FIGURE 5. Survey lines of five marked graves with different burial ages

The horizontal axis reflects the distance (m). Time zero correction, dewow, bandpass Butterworth, gain function and background removal were all used to boost the GPR data. When slice-maps at specific depths in the ground were created, 3-D processing shows the spatial position of amplitudes which can help in subsurface analysis. The amplitudes of radar reflections are gridded and interpolated to create a uniform distribution of radar reflection strengths across the mapped area (Conyers 2013).

## RESULTS

Figure 6 display the findings of the human burial analysis. All observed burials were identified regardless

of their burial's age. When looking for human burials, a GPR device with a 500 MHz central frequency antenna was used because it offers an excellent balance between penetration depth and subsurface feature resolution (Damiata et al. 2013; Schultz et al. 2008). Consequently, the GPR method approach offers comprehensive details on human burial identification.

### PERMATANG PASIR CEMETERY

In the Permatang Pasir, the soil type was a poorly graded of 0% gravel, 98.8% sand and 1.4% silt/clay. On the radar section, the penetration of the 500 MHz GPR antenna was well resolved until 2 m depth. The overall soil profile at Permatang Pasir appeared to be fairly homogeneous.

As a result, defining the hyperbola reflection of human burial in GPR profiles was uncomplicated.

Figure 6 shows eight hyperbolic reflections (G1, G2, G3, G4, G5, G6, G7, G8) shown clearly in the radar section with depth ranging from 0.7 to 1.0 m. These hyperbolic reflections were correctly locating the exact location of the human burials. The most interesting

anomalies were observed at a 5 m distance in Figure 6(a)-6(c)), which was a clear hyperbolic shape. There was no tombstone on the surface, and this anomaly was connected from line 1 until line 3. An unknown burial was thought to be the cause of this anomaly. At 1.6 m deep below the ground surface, a continuous horizontal reflection extends from north to south through the entire section of the most GPR profile.

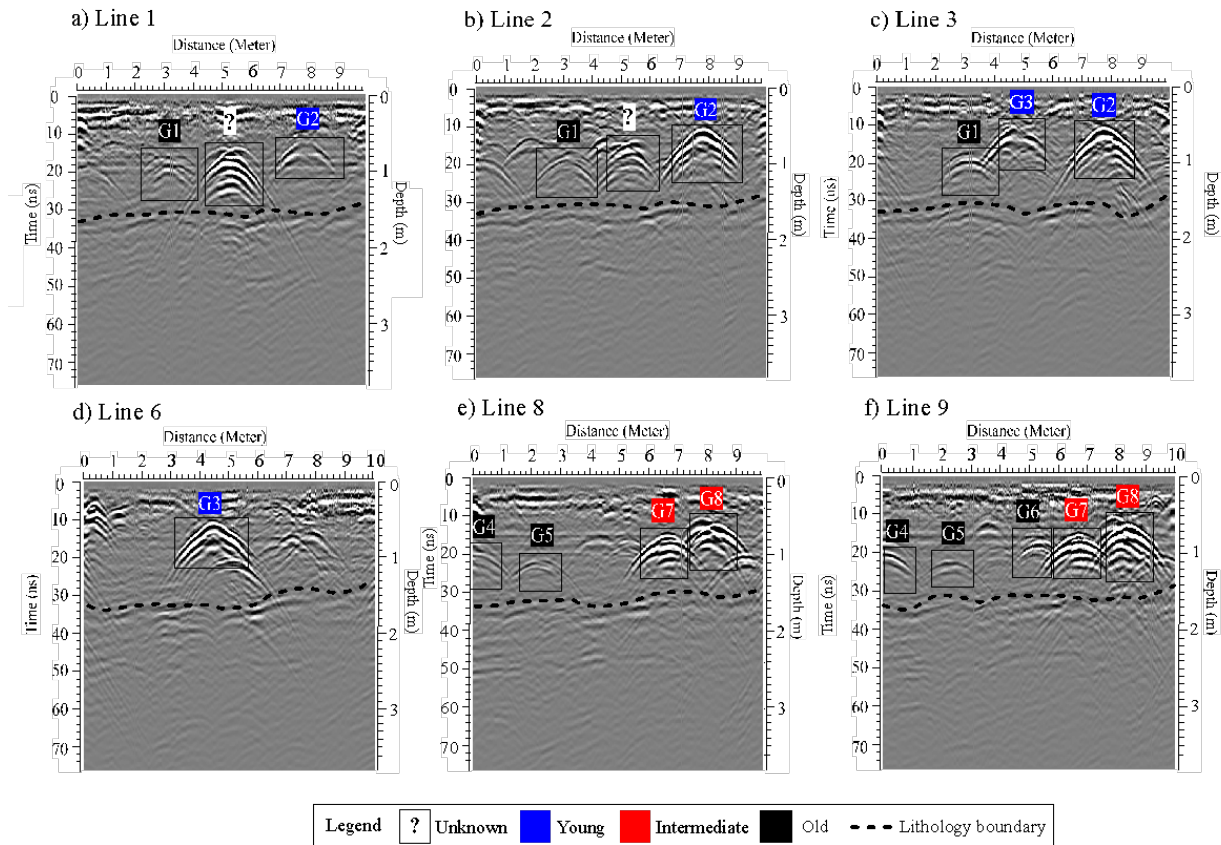


FIGURE 6. Processed 500 MHz 2D GPR profile a) Line 1 b) Line 2 c) Line 3 d) Line 6 e) Line 8 f) Line 9 with target position (black box) and lithology boundary (dotted line)

Based on the markers on the tombstone, the varying reflection strength and polarity towards the human burials were observed and compared to their ages. The age was classified into three categories: young that were <5 years old (G2, G3); intermediate that were 5-50 years old (G7, G8); old that were 50+ years old (G1, G4, G5, G6).

AGE IDENTIFICATION

The basic principle of GPR, focused on reflection strength and polarity, was used to determine the human

burial age. These ages are described in the following sections.

I. YOUNG AGE (G2, G3)

The G2 and G3 burials show strong amplitude reflection with reversed polarity (Figure 7).

AGE INTERMEDIATE (G7, G8)

The G7 and G8 burials were observed with high amplitude reflection and reversed polarity (Figure 8).

#### OLD AGE (G1, G4, G5, G6)

All old burials were shown with low amplitude reflection and normal polarity (Figure 9).

#### UNKNOWN AGE

The unknown burial was observed with high amplitude reflection and reversed polarity.

Meanwhile, the continuous horizontal reflection at 1.6 m depth have the same polarity to the ground reflection.

Time intervals were shown in six sections: 13.3 ns (0.7 m), 16.2 (0.8 m), 19.5 ns (1.0 m), 22.3 ns (1.1 m), 31.1 ns (1.6 m), 35.8 (1.8 m) (Figure 12). From 0.7 to 0.8 m, four anomalies (G2, G3, G7, G8) could be seen clearly, which indicated as young and intermediate burials. However, the majority of old burials (G1, G4, G5, G6) could be seen at 1 m depth, which was deeper than the young and intermediate burials. The unknown burial was discovered at a depth of 0.7 m depth. These anomalies in the time slice corresponds to the hyperbola seen on the radar sections (Figure 6). The continuous horizontal reflection was observed at 31.1 ns (1.6 m) extending from north to south of the slice.

#### TITI TERAS CEMETERY

The soil in Titi Teras was clayey sand, with 0 gravel, 85.4, sand and 14.6% silt/clay. The 500 MHz GPR antenna's penetration was well resolved until 1.2 m depth due to the presence of clay in the study area. Since there was lot of sand and clay in this soil, the chaotic reflection was strong enough to represent this soil type, which had heterogeneous appearance. Therefore, identifying the hyperbola reflection of human burial in GPR profiles was more difficult.

Figure 13 illustrates five hyperbolic reflections (G1, G2, G3, G4, G5) in the radar section at depth ranging from 0.7 to 1.0 m. These hyperbolic reflections were correctly locating the exact location of the graves. At a distance 0 m, the interesting anomaly was observed in Figure 13(a) - 13(d), which was a clear hyperbolic shape. There was no tombstone on the surface, and the anomaly was attached from line 1 to line 4. This anomaly was assumed as an unknown grave. Every profile had tree root reflection, but it was within the 0.4 m depth.

The different reflection strength and polarity towards human burials were observed and correlated to their ages based on the markers on the tombstones. The ages were divided into two categories: young that were <5 years old (G3, G4, G5); old that were 50+ years old (G1, G2).

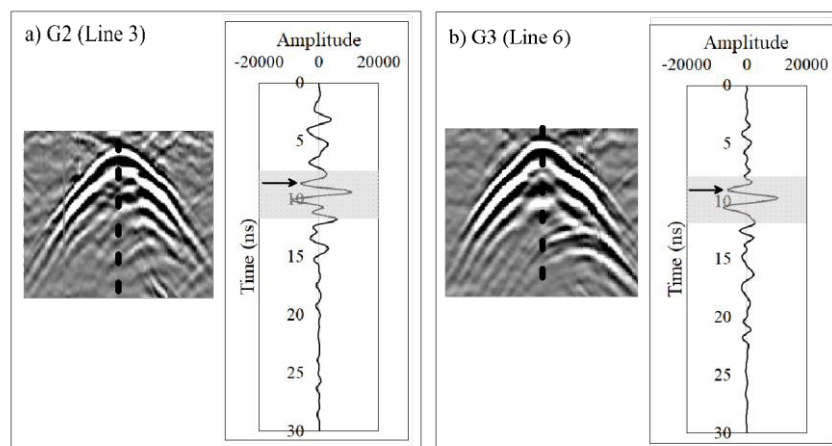


FIGURE 7. Young burial position (dotted line) a) G2 at Line 3 b) G3 at line 6 with target amplitude traces (reversed polarity)

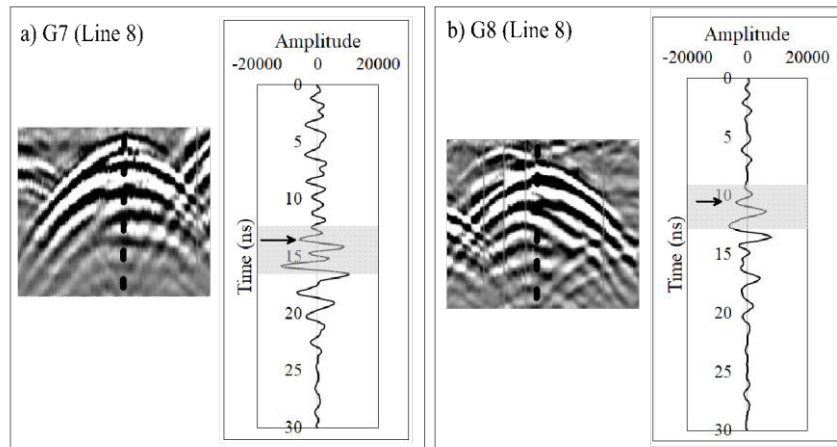


FIGURE 8. Intermediate burial position (dotted line) a) G7 at Line 8 b) G8 at line 8 with target amplitude traces (reversed polarity)

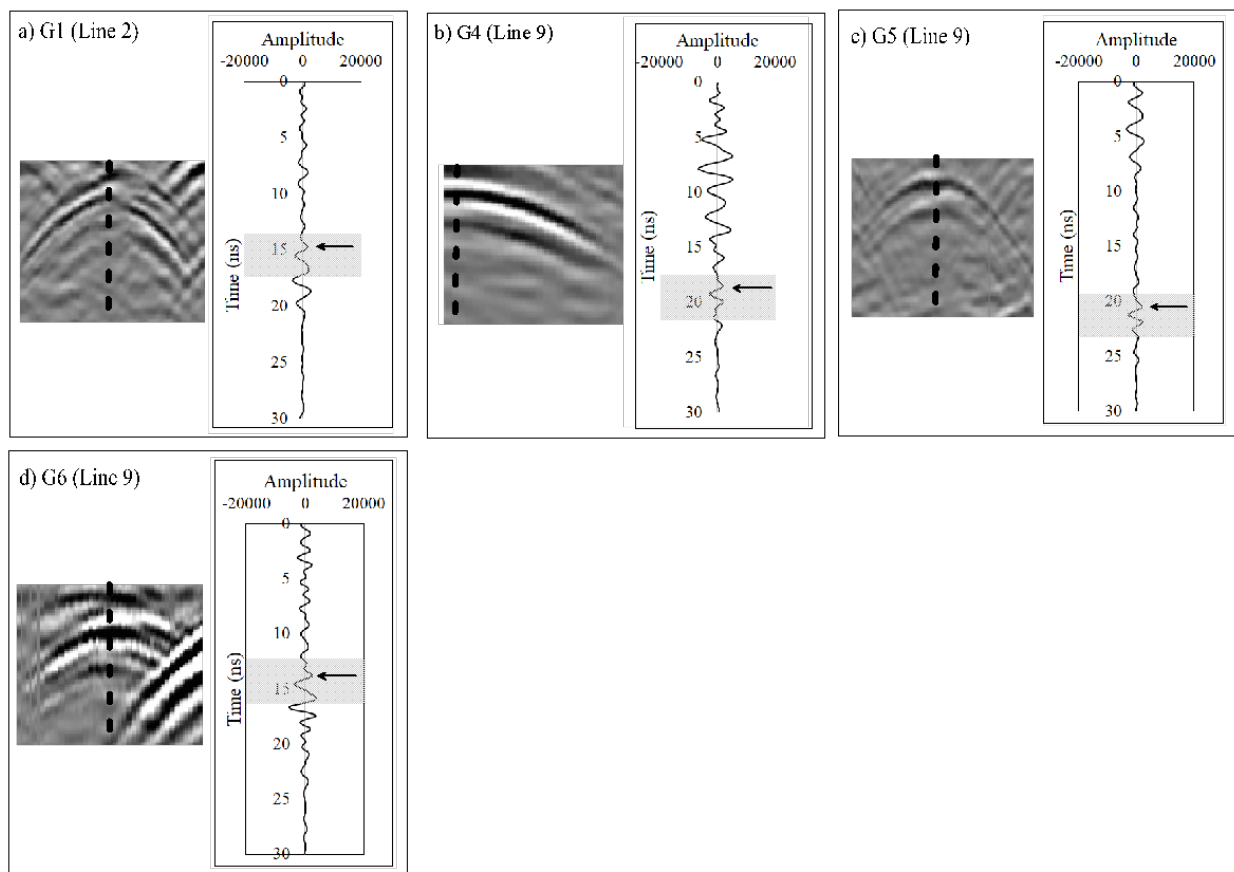


FIGURE 9. Old burial position (dotted line) a) G1 at Line 2 b) G4 at line 9 c) G5 at line 9 d) G6 at line 9 with target amplitude traces (normal polarity)

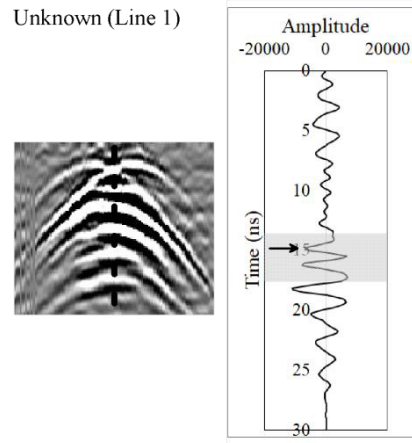


FIGURE 10. Unknown burial position at Line 1 with target amplitude traces (reversed polarity)

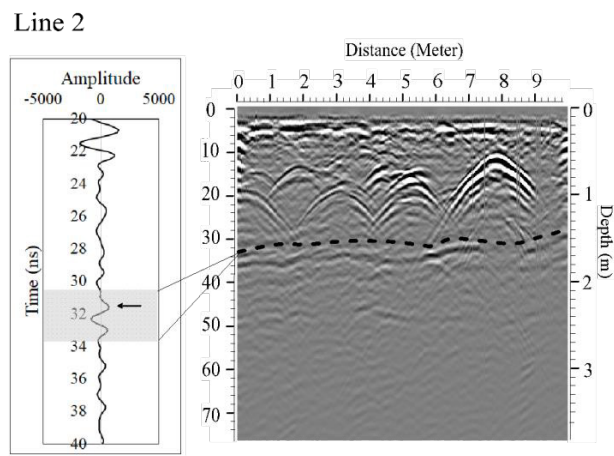


FIGURE 11. Boundary layer (dotted line) with amplitude traces (normal polarity)

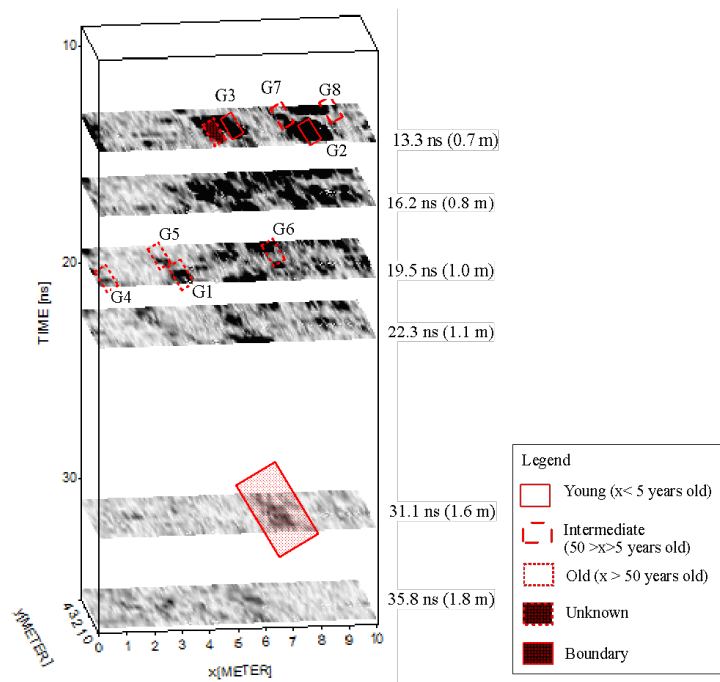


FIGURE 12. Time-slices from a GPR survey of Permatang Pasir cemetery extracted from the travel time: 13.3-35.8 ns in combination with detected graves

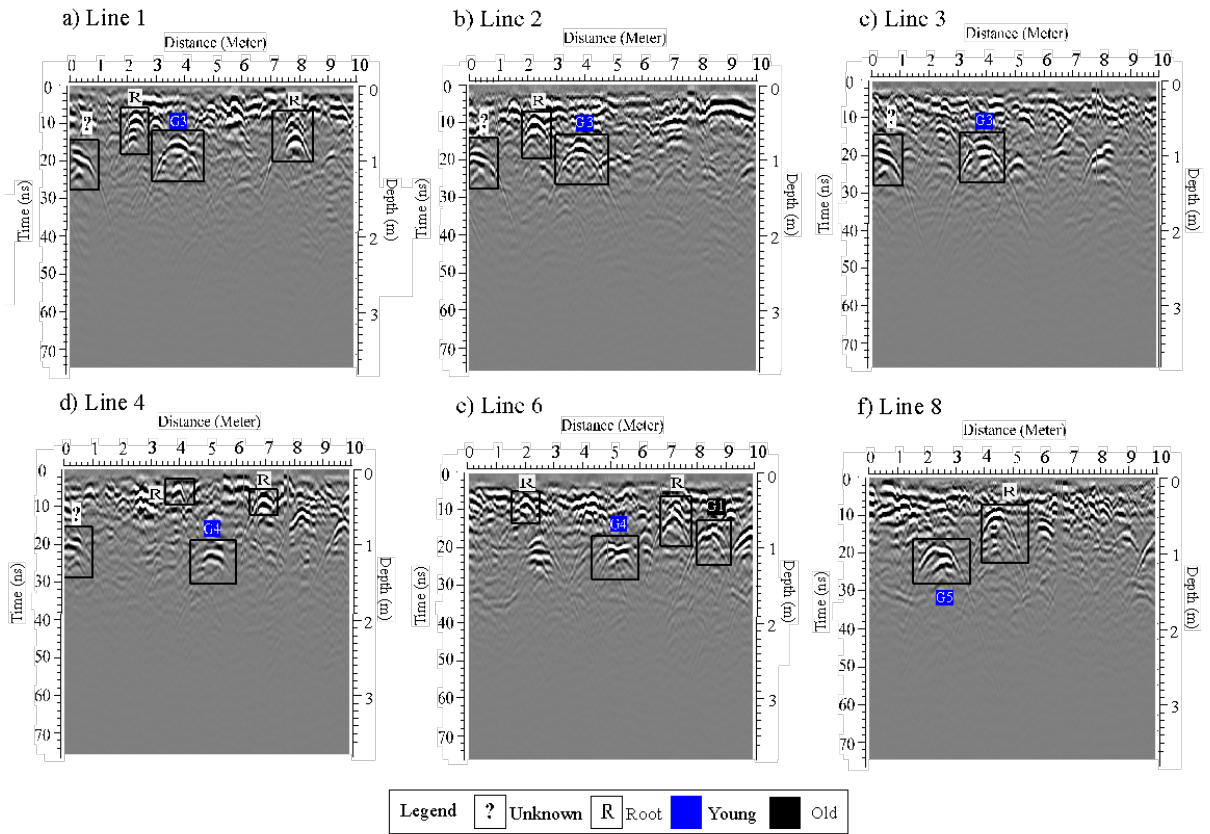


FIGURE 13. Processed 500 MHz 2D GPR profile a) Line 1 b) Line 2 c) Line 3 d) Line 6 e) Line 8 f) Line 9 with target position (black box)

AGE IDENTIFICATION

The basic theory of GPR was used to assess the human burial age, which was dependent on reflection strength and polarity. The following parts go through these ages in detail.

YOUNG AGE (G3, G4, G5)

As shown in Figure 14, the young burials were characterized by high amplitude reflection with reversed polarity.

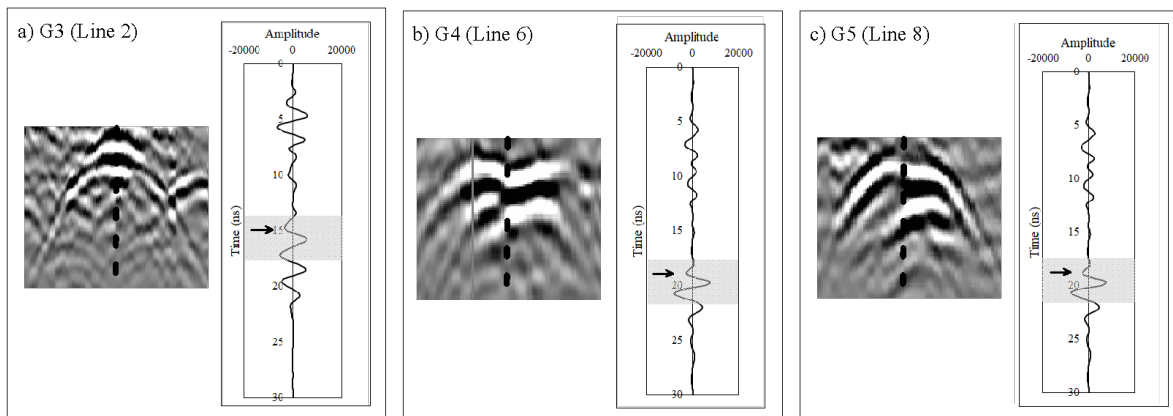


FIGURE 14. Young burial position (dotted line) a) G3 at Line 2 b) G4 at line 6 c) G5 at line 8 with target amplitude traces (reversed polarity)

OLD AGE (G1, G2)

G1 burial was seen at a distance of 8.5 m and was linked to lines 5 and 7. With low amplitude reflection and normal polarity, this old burial was discovered. However, due to very weak amplitude reflection, no G2 burial was found in the GPR profile (Figure 15).

UNKNOWN AGE

The unknown burial was observed with high amplitude

reflection and reversed polarity (Figure 16).

Six sections are represented in Figure 17 from the 0.54 m to 1 m depth. Majority of the human burial were buried between 0.8 and 1.0 m depth, where the amplitude of different detected human burial age can be seen. An old burial (G1) with slightly blurry structure was observed at 0.8 m depth. In comparison, the young and unknown burial were easily mapped and show with a clear anomaly at 0.8 and 1.0 m depth.

G1 (Line 6)

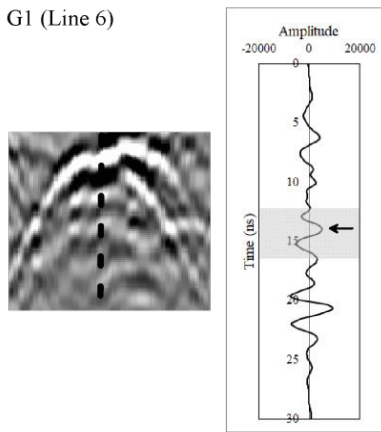


FIGURE 15. Old burial (G1) position at line 6 (dotted line) with target amplitude traces (normal polarity)

Unknown (Line 2)

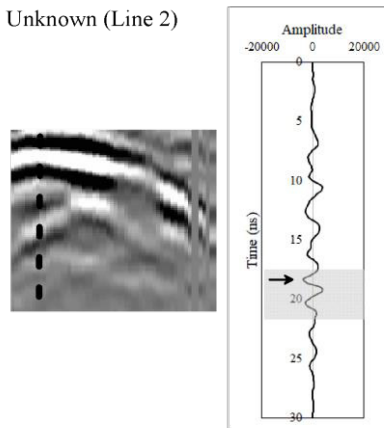


FIGURE 16. Unknown burial position on Line 2 with target amplitude traces (reversed polarity)

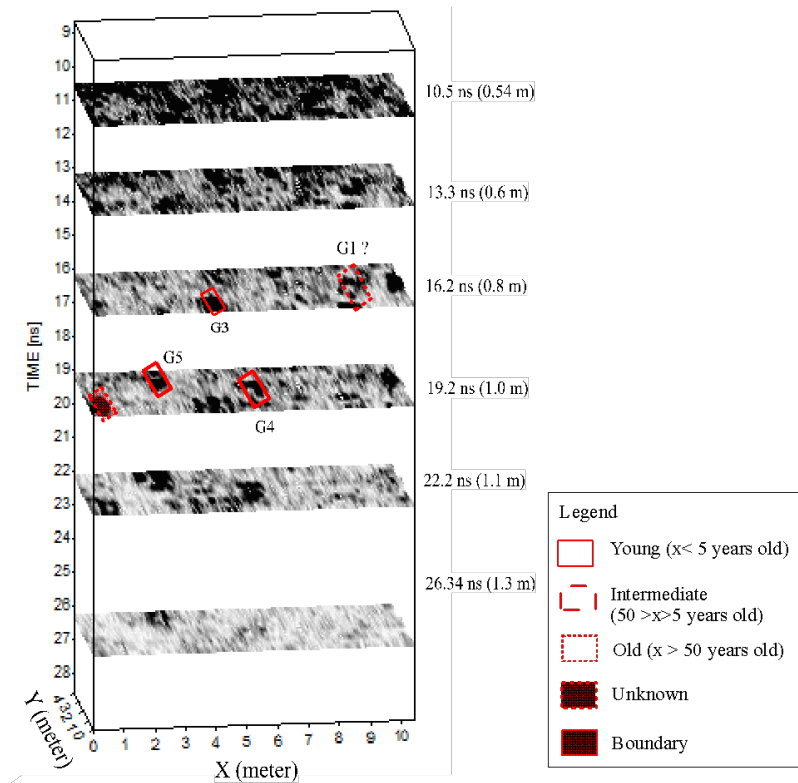


FIGURE 17. Time-slices from a GPR survey of Titi Teras cemetery extracted from the travel time: 10.5-26.34 ns in combination with detected graves

#### DISCUSSION

GPR data can be used to analyze the type of soil and each one has its own geological composition, relative permittivity, and electrical conductivity properties (Saarenketo & Scullion 2000). The electrical conductivity of the soil is a critical factor in determining the attenuation and penetration depth of radar signals. The higher the soil's electrical conductivity, the lower the GPR signal's penetration since the EM energy dissipates more quickly through heat, resulting in a lack of signal intensity at depth. The electrical conductivity of a soil rises as the amount of clay, salinity, and moisture content increases (Abidin et al. 2017; Afshar et al. 2015). Since the Permatang Pasir soils are mainly made up of sands with poor electrical conductivity, the penetration depth was greater than that of Titi Teras soils rich in conductivity materials. Furthermore, since Permatang Pasir soil has fewer signal attenuation, it is also uncomplicated and good environments for GPR investigations, with a homogeneous appearance in GPR profiles. The strongly reflective layers in Titi Teras, may be attributed to high

combination of sand and clay content, resulting in dielectric constant discontinuities in the subsurface and a more heterogeneous or cluttered appearance in GPR profiles.

Various reflection shapes were found (Figures 6 and 12) based on the amplitude and geometries of the reflectors such as planar and hyperbola reflection. As seen in Permatang Pasir profiles (Figure 6), a planar reflection was observed as a different soil type. According to Conyers (2004), hyperbola reflection occurs on the edge of a significant object as a result of a conical radiation pattern generated by the GPR antenna, which radiated outward as it travels deeper in the ground. The radar energy can be reflected by buried objects that are not directly under the antenna. When the antenna is positioned directly on top of the buried object, the exact location and depth are recorded, with the apex reflecting. The arms of the hyperbola represent the reflected energy that traveled the oblique wave direction. Objects in the grave shaft are normally visible as hyperbola reflection, which are produced by coffin tops or sides, void spaces inside intact or partly collapsed coffins and human bodies in the

ground. Usually, bodies will be buried in Permatang Pasir and Titi Teras cemeteries with a wooden coffin and a few wooden board pieces to enclose the body, respectively. Conyers (2004) stated that hyperbola with insufficient multiple reflections below its apexes is usually a wooden coffin or the remaining void spaces from the collapsed coffin. The void spaces in the coffin were assumed to be the broader hyperbola with deficient multiple reflection in Figures 7, 8, and 14. Besides, the reflection of human burials would have a broader hyperbola than other features such as rock and tree roots. Figure 13 shows a few narrower and shallower hyperbola reflection between 0.3 and 0.5 m depths in the Titi Teras, which were reflections from larger tree roots when the GPR antenna passes near the tree.

Reflection polarity provides valuable information about the physical properties of the subsurface that cause reflections. As radar energy is transmitted from a low velocity interface, the polarity of the reflected wave is similar to the direct wave, and this is known as the normal polarity. The soil horizon (Figure 11) in Permatang Pasir and old burials in both study area had normal polarity (Figures 9 and 15). Since soil velocity decreased with depth, the second layer of soil was supposed to be more saturated soil. Meanwhile, the old burials were predicted from the reflection of burial feature or corpse remains. Conversely, when radar energy is transmitted from a high velocity interface, the polarity of the reflection differs from the direct wave and this is referred to as reversed polarity (Conyers 2004; Damiata et al. 2013). The reflections of young and intermediate burials had a reversed polarity, as predicted on void spaces in the grave shaft. The unknown burial was also observed with reversed polarity in both study areas, as assumed by void reflection. The use of polarity reflection changes to detect void spaces beneath the surface has been studied by several authors (Chlaib et al. 2014; Conyers 2015; Damiata et al. 2013).

The identification of human burial reflection can be detected by the contrast in relative permittivity properties of two materials. The greater the relative permittivity contrasts between the buried feature and the surrounding soil, the greater the amount of reflected energy and signal amplitude on the GPR profile. If the relative permittivity of the buried feature and the surrounding soil is similar, majority of the incident wave passes through the interface. As a result, the buried feature will become a low reflector of EM energy and will be difficult to detect on radar section (Bevan 1991; Doolittle 1988; Vaughan 1986). Conyers (2006) claims

that the wooden materials have very poor signals. If an air-filled exists, the GPR response is determined by the difference in relative permittivity between the material contained within the coffin and the surrounding soil. When the coffin is intact, there are a lot of void spaces, which will increase the amplitude value of the burial, as seen in young burials (Figures 7 and 14). This was due to a large difference in relative permittivity between the air and the surrounding soil. However, the intermediate burial reflection was predicted from the collapse of the coffin's void spaces as a result of the lower amplitude reflection compared to the young burials. This was because the wooden coffin decomposes rapidly due to the acid soils and soil pressure (McGowan et al. 2015), which will cause the coffin to collapse within a decade and reducing the void spaces (Doolittle & Bellantoni 2010). The reflection strength for the unknown burial was observed with high amplitude reflection, implying that the remaining void spaces in the grave shaft were retained (Figures 10 and 16). The range of reflection strength for the unknown burial was also similar to the intermediate burial, indicating that the unknown burial was of intermediate age. Due to lower contrast in relative permittivity, the oldest burial has the lowest reflected signal on the radar section. This was due to the fact that the burial feature and corpse would decompose over time, resulting in poor contrasting radar signals and becoming less visible on GPR profiles (Koppenjan et al. 2003).

The type of soil in which the body was buried had the greatest impact on the reflection strength of human burial in this study. According to Doolittle and Bellantoni (2010), the decomposition rate is regulated by the time of burial, soil types, moisture content, burial depth, temperature, and vegetation. Because of the dry soil and no vegetation present in the Permatang Pasir, human burials will last longer (Dupras et al. 2006). Most old burials in Permatang Pasir were buried at a depth of 1 m. It was expected that older burials (Figure 9) would still be visible in the GPR profile due to slower decomposition rates and that deeper burials would be preserved for longer periods of time. Schultz (2008) stated that shallow burials have more oxygenation and rot quicker than deeper burials. Therefore, GPR was unable to detect one old burial (G2) in the Titi Teras cemetery. This study area has a lot of tree and soil conductivity, meaning the corpse can be decompose faster (Dupras et al. 2006).

The spatial position of amplitude in 3-D GPR has been used to improve the visual image and target detection at sites in Permatang Pasir Titi Teras cemetery.

The distribution of amplitude time-slice data may indicate changes in soil properties or the existence of human burial anomalies (Doolittle & Bellantoni 2010). As illustrated in Figures 12 and 17, the young and intermediate burials were clearly observed in both study areas, indicating a good state of preservation and the presence of void spaces in grave shaft. However, older burials do not stand out as clearly as other burial implying that this burial only left the corpse or burial feature behind.

#### CONCLUSION

GPR surveys were carried out at Permatang Pasir and Titi Teras cemetery to locate in varying soil types and burial ages. Due to various types of soil and the surrounding conditions, the surveys yielded significantly different results. The objective of this study was to investigate the use of GPR to detect human burial in sandy and clay sand soil. Second, the results of GPR signals from marked graves with known burial ages will be detailed. Many different bases were used to interpret and describe data anomalies like reflection shape, signal polarity and reflection strength. The penetration depths were 1.8 and 1.3 m for the 500 MHz in Permatang Pasir and Titi Teras cemetery, respectively. In Permatang Pasir, all known graves and one unmarked grave were discovered. In Titi Teras, however, four human burials and one unknown burial were successfully discovered, with the exception of one old burial. Because of the very low reflection strength between the burial feature and the surrounding soil, the old burial is difficult to detect with GPR. The use of 3-D GPR representation has improved the detection of unmarked graves in both study areas.

#### ACKNOWLEDGEMENTS

The author would like to thank the geophysics staff of the Universiti Sains Malaysia, as well as postgraduate students for their precious involvement with geophysics field data acquisition. This research was funded by Universiti Sains Malaysia through the Fundamental Research Grant Scheme (grant numbers 203/PFIZIK/6711683).

#### REFERENCES

- Abidin, M.H.Z., Saad, R., Wijeyesekera, D.C., Ahmad, F., Baharuddin, M.F.T., Tajudin, S.A.A. & Madun, A. 2017. The influences of basic physical properties of clayey silt and silty sand on its laboratory electrical resistivity value in loose and dense conditions. *Sains Malaysiana* 46(10): 1959-1969.
- Afshar, A., Abedi, M., Norouzi, G.H. & Riahi, M.A. 2015. Geophysical investigation of underground water content zones using electrical resistivity tomography and ground penetrating radar: A case study in Hesarak-Karaj, Iran. *Engineering Geology* 196: 183-193.
- Annan, A.P. 2009. Electromagnetic principles of ground penetrating radar. In *Ground Penetrating Radar: Theory and Applications*, edited by Jol, H.M. New York: Elsevier. pp. 1-37.
- Annan, P. 2003. Ground penetrating radar principles, procedures and applications. *Sensors and Software* 2003: 278.
- Baker, G.S., Jordan, T.E. & Pardy, J. 2007. An introduction to ground penetrating radar (GPR). *Special Papers-Geological Society of America* 432: 1-18.
- Bevan, B.W. 1991. The search for graves. *Geophysics* 56(9): 1310-1319.
- Chlaib, H.K., Mahdi, H., Al-Shukri, H., Su, M.M., Catakli, A. & Abd, N. 2014. Using ground penetrating radar in levee assessment to detect small scale animal burrows. *Journal of Applied Geophysics* 103: 121-131.
- Conyers, L.B. 2015. Analysis and interpretation of GPR datasets for integrated archeological mapping. *Near Surface Geophysics* 13(6): 645-651.
- Conyers, L.B. 2013. *Ground Penetrating Radar for Archaeology*. 3<sup>rd</sup> ed. Latham, Maryland: Rowman and Littlefield Publishers. pp. 129-151.
- Conyers, L.B. 2006. Ground-penetrating radar techniques to discover and map historic graves. *Historical Archaeology* 40(3): 64-73.
- Conyers, L.B. 2004. Moisture and soil differences as related to the spatial accuracy of GPR amplitude maps at two archeological test sites. In *Proceedings of the 10<sup>th</sup> International Conferences on Ground Penetrating Radar*. Institute of Electrical and Electronics Engineers (IEEE).
- Damiata, B.N., Steinberg, J.M., Bolender, D.J. & Zoëga, G. 2013. Imaging skeletal remains with ground-penetrating radar: Comparative results over two graves from viking age and medieval churchyards on the stóra-seyla farm, northern Iceland. *Journal of Archaeological Science* 40(1): 268-278.
- Davis, J.L., Heginbottom, J.A., Annan, A.P., Daniels, R.S., Berdal, B.P., Bergan, T., Duncan, K.E., Lewin, P.K., Oxford, J.S., Roberts, N. & Skehel, J.J. 2000. Ground penetrating radar surveys to locate 1918 Spanish flu victims in permafrost. *Journal of Forensic Science* 45(1): 68-76.
- Doolittle, J.A. & Bellantoni, N.F. 2010. The search for graves with ground-penetrating radar in Connecticut. *Journal of Archaeological Science* 37(5): 941-949.
- Dupras, T.L., Schultz, J.J., Wheeler, S.M. & Willimas, L.J. 2006. *Forensic Recovery of Human Remains: Archaeological Approaches*. Boca Raton: CRC Press.
- Fiedler, S., Illich, B., Berger, J. & Graw, M. 2009. The effectiveness of ground-penetrating radar surveys in the location of unmarked burial sites in modern cemeteries. *Journal of Applied Geophysics* 68(3): 380-385.

- Gaffney, C., Harris, C., Pope-Carter, F., Bonsall, J., Fry, R. & Parkyn, A. 2015. Still searching for graves: An analytical strategy for interpreting geophysical data used in the search for “unmarked” graves. *Near Surface Geophysics* 13(6): 557-569.
- Hansen, J.D., Pringle, K.J. & Goodwin, J. 2014. GPR and bulk ground resistivity surveys in graveyards: Locating unmarked burials in contrasting soil types. *Forensic Science International* 237: e14-e29.
- Hassan, K. 1990. A summary of the quaternary geology investigations in Seberang Prai, Pulau Pinang and Kuala Kurau. *Geological Society of Malaysia* 26: 47-53.
- Koppenjan, S.K., Nevada, B., Schultz, J.J., Falsetti, A.B., Collins, M.E., Ono, S. & Lee, H. 2003. The application of GPR in Florida for detecting forensic burials. In *16th EEGS Symposium on the Application of Geophysics to Engineering and Environmental Problems European Association of Geoscientists & Engineers*.
- McGowan, G. & Prangnell, J. 2015. A method for calculating soil pressure overlying human burials. *Journal of Archaeological Science* 53: 12-18.
- Mellett, J.S. 1992. Location of human remains with ground-penetrating radar. In *Proceedings, 4<sup>th</sup> International Conference on Ground Penetrating Radar*. Geological Survey Finland.
- Nazli, H., Bicak, E. & Sezgin, M. 2010. Experimental investigation of different soil types for buried object imaging using impulse GPR. In *Proceedings of the XIII International Conference on Ground Penetrating Radar*, Institute of Electrical and Electronics Engineers (IEEE).
- Neal, A. 2004. Ground penetrating radar and its use in sedimentology: Principles, problems and progress. *Earth-Science Reviews* 66(3-4): 261-330.
- Nobes, D.C. 2000. The search for “Yvonne”: A case example of the delineation of a grave using near-surface geophysical methods. *Journal of Forensic Sciences* 45(3): 715-721.
- Nobes, D.C. 1999. Geophysical surveys of burial sites: A case study of the Oaro Urupa site. *Geophysics* 64(2): 357-367.
- Ruffell, A. 2005. Searching for IRA “disappeared”: Ground-penetrating radar investigation of a churchyard burial site, Northern Ireland. *Journal of Forensic Science* 50(6): 1430-1435.
- Saarenketo, T. & Scullion, T. 2000. Road evaluation with ground penetrating radar. *Journal of Applied Geophysics* 43(2-4): 119-138.
- Schultz, J.J. 2008. Sequential monitoring of burials containing small pig cadavers using ground penetrating radar. *Journal of Forensic Science* 53(2): 279-287.
- Schultz, J.J. 2007. Using ground-penetrating radar to locate clandestine graves of homicide victims: Forming forensic archaeology partnerships with law enforcement. *Homicide Studies* 11(1): 15-29.
- Vaughan, C.J. 1986. Ground penetrating radar surveys used in archaeological investigations. *Geophysics* 51(3): 595-604.
- Widodo, W., Aditama, I.F., Syaifullah, K., Mahya, M.J. & Hidayat, M. 2016. Detecting buried human bodies using ground penetrating radar. *Earth Science Research* 5(2): 59-68.

Geophysics Program  
School of Physics  
Universiti Sains Malaysia  
11800 USM, Pulau Pinang  
Malaysia

\*Corresponding author; email: nurazwin@usm.my

Received: 2 October 2020

Accepted: 7 June 2021